Speckle reduction with attenuation compensation for Skin OCT images enhancement

Mohammad R. N. Avanaki and Ali Hojjat

University of Kent, Canterbury, CT2 7PD, United Kingdom

Abstract. The enhancement of skin image in optical coherence tomography (OCT) imaging can help dermatologists to investigate tissue layers more accurately, hence the more efficient diagnosis. In this paper, we propose an image enhancement technique including speckle reduction, attenuation compensation and cleaning to improve the quality of OCT skin images. A weighted median filter is designed to reduce the level of speckle noise while preserving the contrast. A novel border detection technique is designed to outline the main skin layers, stratum corneum, epidermis and dermis. A model of the light attenuation is then used to estimate the absorption coefficient of epidermis and dermis layers and compensate the brightness of the structures at deeper levels. The undesired part of the image is removed using a simple cleaning algorithm. The performance of the algorithm has been evaluated visually and numerically using the commonly used no-reference quality metrics. The results shows an improvement in the quality of the images.

Keywords: Optical coherence tomography (OCT), Skin, Image enhancement, Speckle reduction, Attenuation compensation.

1 Introduction

Optical coherence tomography (OCT) is an advanced high resolution non-invasive imaging tool involving both morphological and optical properties, which delivers three-dimensional (3D) images from the microstructure compartments within skin tissue [1-2]. OCT images are constructed by measuring the backscattered signal from different depths within the skin at different transverse positions [3]. The amplitude and phase of the back scattered signal is changed regarding to the colour/depth, and morphological structure of the organelles which correspond to the two major optical characteristics of material known as absorption and scattering coefficients, respectively. Therefore, OCT has become the favourable device for investigating changes in morphological microstructure of the skin [3]. OCT, like other imaging technique based on the detection of coherent waves, are subject to significant presence of speckle noise [4]. The other major issue is the tissue absorption which results in a weak back scattered signal from deeper tissue layers. The absorption within the skin is mainly due to haemoglobin, melanin and water content[1].

The development of successful speckle noise reduction algorithms for OCT is particularly challenging. Many methods have been investigated for the reduction of speckle in OCT images using hardware modifications [4] and different image processing algorithms like adaptive digital filtering [5-6], wavelet analysis [5,7], and averaging in time and frequency domain [8]. Based on the behaviour of turbid tissue against the incidence light, we design a weighted median filter to reduce the level of speckle noise in OCT image.

Image enhancement for OCT images can be achieved via hardware modifications as well as signal and image processing approaches. The authors in [9] employed electro-optical phase modulator to increase the sensitivity of the Fourier domain OCT images via the elimination of low-frequency noises from DC and autocorrelation terms. Osmotic agents have been used in [10] to concurrently improve the penetration depth as well as the image contrast in OCT images. Kulkarni et.al. have utilized a linear shift invariant model with the iterative deconvolution to sharpen the OCT images [11]. A review of image processing techniques used for OCT images enhancement is presented by Rogowska and Brezinski [12].

To improve the quality of the OCT skin images, an enhancement algorithm is proposed in which OCT signal attenuation is compensated with regard to an estimate of the absorption coefficients at each skin layer. In addition to image enhancement, supplementary quality improvement is achieved using a cleaning algorithm which eliminates the disturbing signal in the free space between the objective lens and specimen. This signal is the result of scaling after inverse Fourier transform and resampling in the Fourier domain OCT [13].

Material and methods

2.1. OCT system configuration

In this study a swept-source Fourier domain OCT from Michelson Diagnostic TM has been employed for imaging. The OCT, is based on multi beam technology with the focus depth of 0.25mm for four consecutive depths providing the total focal range of 1mm, which produce 7mm x 2mm B-Scans. The lateral and axial resolutions of the OCT are 7.5 μm and 10 μm, respectively. The SLD works with the peak power of 15mW in the central wavelength of 1305nm and with the laser wavelength sweep range of 150nm. Typical penetration depth is 1.5mm.

2.2 Image processing techniques

The enhancement algorithm has three steps; speckle reduction, attenuation compensation, and cleaning. The following sections explain each of the three stages in details.

2.2.1 Speckle reduction algorithm

In OCT, the multiple scattering within the tissue results in unwanted back reflection light generating speckle noise. As the backscattering signal generated by the neighbouring ultrastructures has a random nature with different effect on the measured signal at a specific position, a weighted median filter of signals at the point and its immediate layers which interact more with the layers could be used to estimate the signal. A weighted combination of pixel values I(i,j), I(i,j-1), I(i-1,j-1), I(i-1,j), I(i-1,j+1), and I(i,j+1) is used to estimate the value for pixel I(i,j). This scheme has been considered as the immediate neighbouring pixels at above the current pixel which are most likely to be involved in the generation of the back reflection signal in pixel position (i, j). We used double weighting for pixel (i,j) as the probability of involvement of this pixel should be higher than that of the neighbouring pixels. A weighted median filter is designed to decrease the level of speckle noise while preserving the contrast in the image.

2.2.2 Attenuation modelling and compensation

Beer–Lambert law relates the absorption of light to the property of the material through which the light is travelling [14]. The variation of light optical power versus the travelled path length is exponential. The relation between back reflection light, I, with the incident light, I_0, is given by $I = I_0 e^{-\mu_a L}$, where L is the optical path length and μ_a is absorption coefficient of the specimen [14]. For a specimen consisting of particles with a particular geometrical size, the absorption coefficient can be described as a product of effective cross-section of the particle and the density of chromophors. Effective cross section is directly proportional to the absorption efficient and the geometrical size of the chromophors [15]. For attenuation modelling within the skin, the locations of skin layers are detected and the absorption coefficient for each layer is estimated. The signal attenuation for each layer is then compensated using the coefficient in the layer.

Skin layer detection algorithm
Skin is made up of three main layers, epidermis, dermis, and subcutaneous, which may not be distinct even in normal cases [2]. The skin layers are extracted from the OCT image by searching for the most probable maximum and minimum positions among the local extremums along each A-line profile.

Forward back reflection from stratum corneum results in a high intensity signal at the first layer, top part of the image. Canny gradient algorithm with a high threshold is used to detect the stratum corneum layer. The gradient points obtained are connected using morphological operations, opening and closing, with a horizontal line kernel of size 4 micron.

To find dermis, local maxima[1] are obtained from the smoothed profile of each A-line individually starting from stratum corneum. The number of maxima in the neighbourhood of each pixel is counted and is shown as the value of the pixel. Therefore, the resulting image shows the occurrence of the local peaks in the neighbouring A-lines to the pixel. The accumulative occurrence of peak (AOP) image is then obtained to provide a more stable representation of the location of the local peak for each profile in the image. The position of each locally maximum peak corresponds to the position of changes in tissue characteristics represents the boundary between two different layers. We find the maximum point along each column (A-line) of the AOP image using a median operation. As the boundary between dermis and epidermis is not very clear and there is a transition from one layer to another, we detect the end of epidermis and then use the distance to apply a different absorption coefficient. We, therefore, use the same algorithm to the inverted image to find the most probable position of minima, representing the end of epidermis. The area between the minimum and the maximum lines is considered as the transition area.

Absorption coefficient

[1] In this section, we talk about the position rather than the intensity value of maxima.

Using the intensity change along the tissue, an absorption coefficient is calculated. This is performed for each region, epidermis, and dermis, and the transition area separately. To achieve this, the minimum distance between each two edges for each segment is computed. Pixels horizontally are averaged in each segment along their upper edge, which results one columnar profile for each segment. As OCT imaging system converts the signal using logarithmic function before constructing the image, the effect of attenuation on intensity is linear. Therefore, a linear function, $f(x) = ax + b$, can be fitted to each profile to represent the attenuation by the gradient, a. We use a linear least square's curve fitting algorithm based on Levenberg-Marquardt algorithm (LMA) [16] to extract an average a for each layer. For segments #1 and #3 the coefficients α_1 and α_3 are calculated. Assuming that the segment #2 is a mixture of segment #1 and #3, e.g. having characteristics of both dermis and epidermis, the absorption coefficient of this segment is estimated by average of the absorption coefficients of the two neighbouring layers given by $\alpha_2 = (\alpha_1 + \alpha_3)/2$.

Attenuation compensation

The scheme given in Figure 1, describes the attenuation model of an A-line for the human skin. Having the absorption coefficients for each segment, we can compensate the signal attenuation. This is performed in three steps using the formulation as a function of depth and the absorption coefficients computed for each segment.

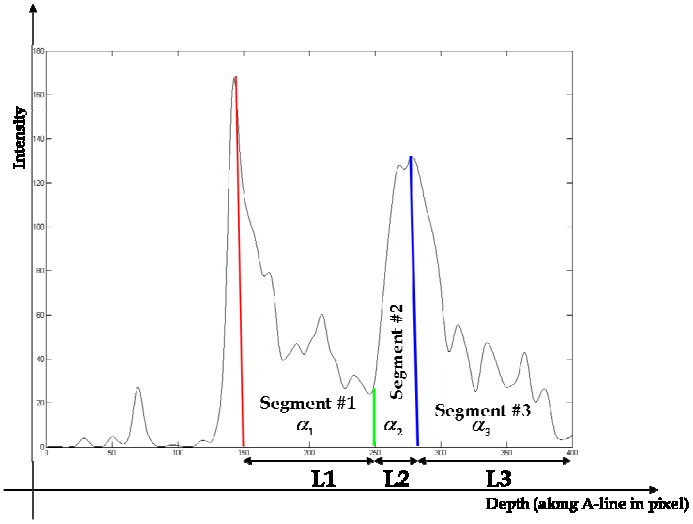

Figure 1. A-line intensity profile for skin. The three segments represent changes in absorption coefficient. Red, green, and blue lines represent estimated position of start of stratum corneum, epidermis and dermis layers in the current A-line.

The back reflected light from the first segment passes just through the first segment, hence, only α_1 should be taken into account as compensation coefficient for this layer. This compensation is applied for the segment #1 and formulated in (1). In equation (1), $I_{old}(i, j)$ is the original intensity value of each pixel, $I_{compensated}(i, j)$ is the attenuation-compensated intensity of each pixel, and $scale$ is a constant representing the distance from the image plane to the sample plane. z is the depth of a pixel in the current segment from the start of the layer.

$$I_{compensated}(i, j) = I_{old}(i, j) + I_{old}(i, j) \times scale \times (\alpha_1 \times z) \quad (1)$$

The back reflected signal from segment #2 passes through the segment #1, therefore compensates the effect of attenuation in segment #2. The length of the segment #1 with the absorption coefficient α_1 should be considered for the next layers. Considering the depth of the pixel in segment #2 with its absorption coefficient α_2, we can write.

$$I_{compensated}(i, j) = I_{old}(i, j) + I_{old}(i, j) \times scale \times (\alpha_1 \times L_1 + \alpha_2 \times z) \quad (2)$$

Likewise for the segment #3, the effect of absorption in the segments #1 and #2 plus absorption in the segment#3 corresponding to the depth of the pixel are considered in (3).

$$I_{compensated}(i, j) = I_{old}(i, j) + I_{old}(i, j) \times scale \times (\alpha_1 \times L_1 + \alpha_2 \times L_2 + \alpha_3 \times z) \quad (3)$$

2.2.3 Cleaning algorithm

In OCT imaging, a perturbation on the signal exists in the space between the specimen and the objective lens due to the scaling procedure, resulting in noisy pixels at the top of the B-scan image. We used an algorithm to remove theses unwanted signals. We applied Canny algorithm to the enhanced image to find the high gradient pixels (strong edge) at the top of the image. The image is scanned in each column till a strong edge is detected. Then the intensity of the scanned pixels are replaced by the minimum value of the scanned-pixels.

3 Results and discussion

The algorithm is applied on thirty five different fingertip images acquired using a swept-source Fourier domain OCT described in Section 2.1. The images are from healthy individuals with three different skin types including light black skin (type5), Caucasian skin (type 1-2), and normal white skin (type3-4).

The result of the proposed layer detection algorithm applied on six finger tip skin is shown in Figure 2. The detected boundaries between different layers are shown in different colours. Given the detected boundaries, we can assume that the stratum corneum starts at the red, epidermis layer is between the red to green lines and dermis is after the blue line. The layer between green and blue line is the transient area.

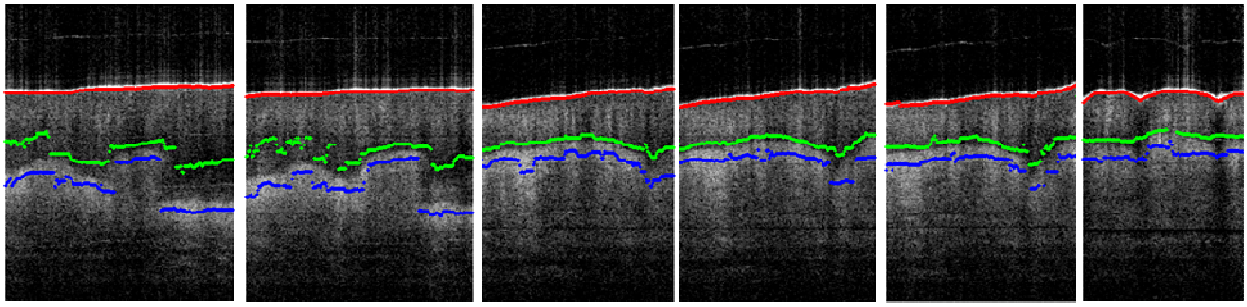

Figure 2. The result of applying the layer detection stage on six fingertip images shown in red, green and blue. The boundaries correspond to the boundary between the three segments in A-line profile described in Figure 1.

The enhancement technique then applied on the skin images. A sample original image and the result of applying every stage of the algorithm, despeckling, enhancement, and cleaning are shown in Figure 3 (a-d), respectively.

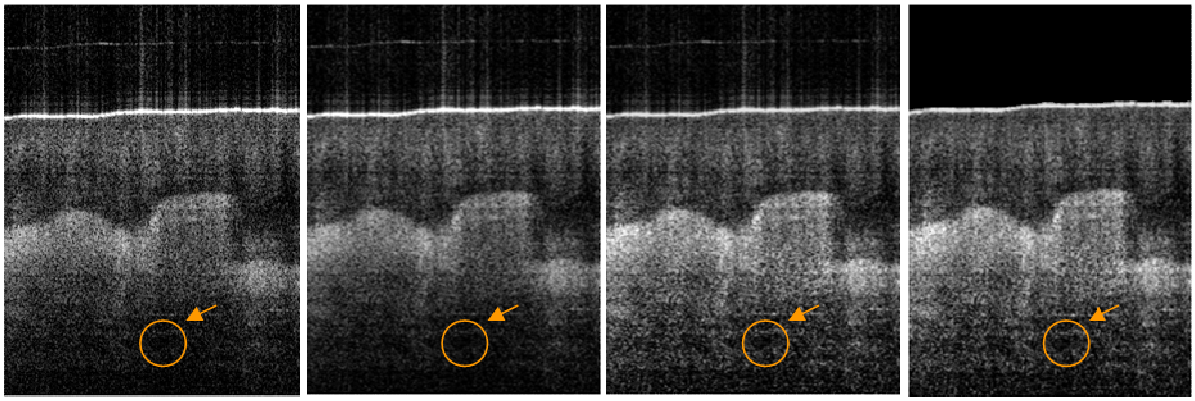

(a) **(b)** **(c)** **(d)**

Figure 3. (a) OCT B-scan of 33-years-old light black finger tip skin (type 5) image taken in-vivo; the size of the specimen is 1.24mm x 1.6 mm equal to 300 x 400 pixel. (b) Image after despeckling algorithm. (c) Despeckled image after attenuation compensation (enhanced image) (d) Enhanced image after cleaning. The orange arrow shows an artery within the dermis which is clearer in the enhanced image.

As seen in Figure 3. (b), the granular artefact of speckle has been reduced while the contrast information of image preserved. The contrast of the image has been increased which produces the brighter and darker areas in the corresponding bright and dark area, respectively. This contrast becomes very important when cancerous aggregation creates a dark area within the skin image and needs to be detected with its border [1-3].

In this study two commonly used No-reference metrics including Signal-to-Noise Ratio (SNR) and Contrast Noise Ratio (CNR) are used for quantitative evaluation. CNR is a measure which shows the difference of an interested area of the image to the whole image and SNR represents the variance of a pixel value in the background noise. The graphs show improvement in both SNR and CNR for the enhanced image as compared with the original image.

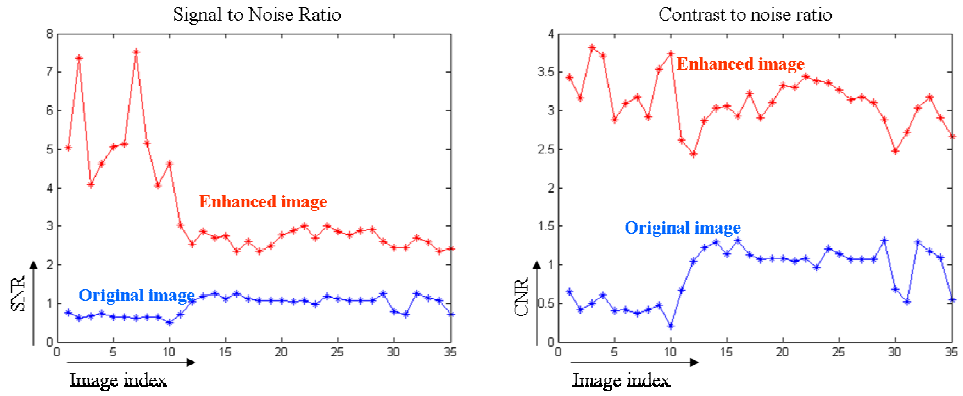

Figure 4. ENL and SNR graphs for original and enhanced mages.

4 Conclusion:

The enhancement of OCT skin images is performed using a multistage algorithm starting with speckle reduction followed by an estimation of the absorption coefficient for different layers used to compensate the intensity and a cleaning stage. The skin layer detection plays an important role as the profiles of the segments are used to estimate the attenuation coefficients. Both qualitative (Figure 4) and quantitative (Figure 3) evaluation of the results tested on 35 images show a reasonable improvement in the OCT images. The enhanced image appears to have higher contrast and less speckle noise. The resultant images can help dermatologist to make a better decision in skin diagnosis..

References

1. A. M. Schmitt, "Principles and Application of Optical Coherent Tomography in Dermatology." *Dermatology*, vol. 217, pp. 12, 2008
2. J. Welzel, "Optical coherence tomography in dermatology: a review," *Skin Res. Technol.*, vol. 7, pp. 1-9, Feb. 2001
3. A. G. Podoleanu, "Optical coherence tomography," *Br. J. Radiol.*, vol. 78, pp. 976-988, Nov. 2005
4. A. Ozcan, A. Bilenca, A. E. Desjardins, B. E. Bouma and G. J. Tearney, "Speckle reduction in optical coherence tomography images using digital filtering," *Scanning*, vol. 20, pp. 27-30, 2007
5. M. Bashkansky and J. Reintjes, "Statistics and reduction of speckle in optical coherence tomography," *Opt. Lett.*, vol. 25, pp. 545-547, 2000
6. J. Rogowska, M. Brezinski, M. L. H. BIC and M. Belmont, "Evaluation of the adaptive speckle suppression filter for coronary optical coherence tomography imaging," *IEEE Trans. Med. Imaging*, vol. 19, pp. 1261-1266, 2000
7. D. C. Adler, T. H. Ko and J. G. Fujimoto, "Speckle reduction in optical coherence tomography images by use of a spatially adaptive wavelet filter," *Opt. Lett.*, vol. 29, pp. 2878-2880, 2004
8. B. Sander, M. Larsen, L. Thrane, J. Hougaard and T. Jorgensen, "Enhanced optical coherence tomography imaging by multiple scan averaging," *Br. Med. J.*, vol. 89, pp. 207-212, 2005
9. J. Zhang, J. S. Nelson and Z. Chen, "Removal of a mirror image and enhancement of the signal-to-noise ratio in Fourier-domain optical coherence tomography using an electro-optic phase modulator," *Opt. Lett.*, vol. 30, pp. 147-149, 2005
10. R. K. Wang, X. Xu, V. V. Tuchin and J. B. Elder, "Concurrent enhancement of imaging depth and contrast for optical coherence tomography by hyperosmotic agents," *Journal of the Optical Society of America B*, vol. 18, pp. 948-953, 2001
11. M. D. Kulkarni, J. A. Izatt and M. V. Sivak, *Image Enhancement in Optical Coherence Tomography using Deconvolution*, 1999
12. J. Rogowska and M. E. Brezinski, "Image processing techniques for noise removal, enhancement and segmentation of cartilage OCT images," *Phys. Med. Biol.*, vol. 47, pp. 641-656, 2002
13. Y. Feng, R. K. Wang and J. B. Elder, "Theoretical model of optical coherence tomography for system optimization and characterization," *Journal of the Optical Society of America A*, vol. 20, pp. 1792-1803, 2003.
14. C. BOHREN and D. HUFFMAN, "Absorption and scattering of light by small particles," *Research Supported by the University of Arizona and Institute of Occupational and Environmental Health.New York, Wiley-Interscience, 1983, 541 p*, 1983
15. W. Cheong, S. Prahl and A. Welch, "A review of the optical properties of biological tissues," *Quantum Electronics, IEEE Journal of*, vol. 26, pp. 2166-2185, 1990
16. W. Yang, W. Cao, T. S. Chung and J. Morris, *Applied Numerical Methods using MATLAB*. J. Wiley Hoboken, NJ, 2005